New type of charged Q-ball dark matter in gauge mediated SUSY breaking models

Jeong-Pyong Hong and Masahiro Kawasaki

Institute for Cosmic Ray Research, The University of Tokyo, 5-1-5 Kashiwanoha, Kashiwa, Chiba 277-8582, Japan
and Kavli IPMU (WPI), UTIAS, The University of Tokyo, 5-1-5 Kashiwanoha, Kashiwa 277-8583, Japan

We examined the viability of a new type of charged Q-ball dark matter scenario. We considered the case where the relics can be treated as ordinary ions, to which we applied the observational constraint from the MICA experiment, where no trail of heavy ionlike object is observed in 10^9 year-old ancient muscovite mica. We have found that the allowed parameter region exists but is smaller than the neutral Q-ball dark matter case. We have also discussed whether our scenario is actually consistent with Affleck-Dine mechanism.

I. INTRODUCTION

The Affleck-Dine mechanism [1] is one of the promising candidates for baryogenesis based on supersymmetric (SUSY) theories, where baryon asymmetry is generated by the dynamics in the phase direction of a baryonic scalar field (called the Affleck-Dine field) such as a squark. After the baryon number generation, the spatial inhomogeneities of the Affleck-Dine field due to quantum fluctuations grows exponentially into nontopological solitons, which are called Q-balls [2–4]. A Q-ball is defined as a spherical solution in a global $U(1)$ theory which minimizes the energy of the system with fixed $U(1)$ charge [5]. The baryon number generated in Affleck-Dine mechanism is confined inside Q-balls. Although Q-balls are stable against decay into squarks, they may gradually decay into quarks and/or leptons, so that the baryon asymmetry in the Universe is generated by quarks emitted from the Q-balls. However, in gauge mediated SUSY breaking models, a baryonic Q-ball can be stable against decay into nucleons [6], while a leptonic Q-ball can decay into leptons.

In the previous work [7], we focused on gauge-mediation-type Q-balls that carry both baryon and lepton charges which can be formed after the Affleck-Dine baryogenesis with $u^c u^c d^c e^c$ flat direction, for instance. We found that the Q-balls can be electrically charged, which are called charged or gauged Q-balls [8], and the charged Q-balls are stable by virtue of the stability of the baryonic component. Thus, the charged Q-ball can be the dark matter in the present Universe. Since the charged Q-balls capture the charged particles, they form ionlike objects which make different experimental signatures compared to the ordinary neutral Q-balls. For instance, Q-balls can be detected by Super-Kamiokande [9,10] or IceCube [11], which probe KKST process [12] where the Q-ball absorbs quarks and emits pions of energy ~ 1 GeV. However, the charged Q-ball relics experience the ordinary electromagnetic processes as well. Thus, the experiments such as MACRO and MICA that can detect those processes are useful to set upper bounds on the flux of the charged Q-balls [9]. The most stringent constraint comes from the MICA experiment [13], where the trail of the heavy ionlike object is not observed in 10^9 year-old ancient mica crystals. Since the observation time is equal to the age of the mica, the constraint on Q-ball flux is much severer than those coming from other experiments. In the previous work [14], we found that the MICA constraint is more stringent than that from IceCube, etc. and allowed region of the model parameters for gauge-mediation-type charged Q-ball dark matter becomes smaller than the neutral Q-ball case.

While the gauge-mediation-type Q-ball is realized when the gauge mediation effect dominates the potential of the Affleck-Dine field, gravity mediation effect may still dominate over the gauge mediation effect if the field value is sufficiently large. In that case, Q-balls with different properties are formed, which we call the new type (or hybrid) Q-balls. In this paper, we assume that the new type of Q-balls are formed, instead of the gauge-mediation-type Q-balls, after the Affleck-Dine mechanism, and investigate whether there exists the allowed parameter region for the new type of charged Q-ball dark matter. Specifically, we apply the MICA constraint on the relics from the new type of charged Q-balls and find the constraint on gravitino mass (SUSY breaking scale) and reheating temperature.

II. NEW TYPE OF Q-BALL

In MSSM, there are numerous flat directions such as $u^c d^c d^c$, and $u^c u^c d^c e^c$, for instance. We consider the dynamics of one of these flat directions in the MSSM. In particular, we consider a flat direction with nonzero baryon and lepton charges, which we call the Affleck-Dine field.

In our Universe, the supersymmetry is broken, so the flat directions obtain soft SUSY breaking terms. We consider the minimal gauge mediation model [15–17], where SUSY is spontaneously broken by F-term of a singlet field Z:

$$\langle F_Z \rangle = F \neq 0. \tag{1}$$

The soft breaking effect is mediated to the visible sector by messenger fields Ψ and $\bar{\Psi}$, which is a pair of some representations and anti-representations of the minimal GUT group $SU(5)$, via the following interactions:

$$W = kZ\bar{\Psi}\Psi + M_{\mathrm{mess}}\bar{\Psi}\Psi, \tag{2}$$

where k and M_{mess} denote a Yukawa constant and messenger mass, respectively.

Then, the Affleck-Dine field obtains the following potential [2,18,19] by the breaking effect above:

$$V = V_{\mathrm{gauge}} + V_{\mathrm{grav}}$$
$$= M_F^4 \left(\log\left(\frac{|\Phi|^2}{M_{\mathrm{mess}}^2}\right) \right)^2 + m_{3/2}^2 \left(1 + K \log\left(\frac{|\Phi|^2}{M_*^2}\right) \right) |\Phi|^2$$
$$+ (\text{A-term}). \tag{3}$$

The first term comes from gauge mediation effect and gauge mediation parameter M_F is defined by

$$M_F \simeq \frac{\sqrt{gkF}}{4\pi} \tag{4}$$

where g generically denotes the gauge coupling of the standard model [18]. The second term originates from gravity mediation effect and the gravitino mass $m_{3/2}$ is given as

$$m_{3/2} \equiv \frac{F}{\sqrt{3}M_P}, \tag{5}$$

where $M_P = 2.4 \times 10^{18}$ GeV is the reduced Planck mass. Here we assume $m_{3/2} < 1$ GeV. The parameter K is a constant which comes from the beta function of mass of the AD field and is typically negative, satisfying $0.01 \lesssim |K| \lesssim 0.1$, and M_* means the renormalization scale. The third term (A-term) is a B and CP violating term which induces the Affleck-Dine rotation.

During inflation, the AD field additionally obtain a negative Hubble induced mass term $-c_H H^2 |\Phi|^2$ due to the coupling to the inflaton, which gives AD field a large vacuum expectation value (VEV). However, after inflation, the Hubble rate becomes smaller than the soft mass and the AD field starts the oscillation around the origin. Then, the spatial inhomogeneities of the AD field, which originate from quantum fluctuations, grow exponentially and form Q-balls. As mentioned in the previous section, the new type of Q-ball [20] is formed if V_{grav} dominates the potential when the AD field starts the oscillation. The condition for the V_{grav} domination is given by

$$\phi_{\mathrm{osc}} > \phi_{\mathrm{eq}} \simeq \sqrt{2}M_F^2/m_{3/2,} \tag{6}$$

where $\phi \equiv \sqrt{2}|\Phi|$, and ϕ_{osc} is the field value at the beginning of the oscillation. A typical charge of the new type of Q-ball can be estimated by a linear approximation or numerical simulations, which is given by [20]

$$Q = \beta \left(\frac{\phi_{\mathrm{osc}}}{m_{3/2}} \right)^2. \tag{7}$$

Here $\beta = 0.02$, which is a numerical constant.

The profile of the new type of Q-ball solution is known to be Gaussian as

$$\phi \propto \exp(-r^2/R_Q^2), \tag{8}$$

and the mass, size, and mass per unit charge of the new type of Q-ball are given by

$$M_Q \simeq m_{3/2}Q \tag{9}$$

$$R_Q \simeq |K|^{-1/2}m_{3/2}^{-1} \tag{10}$$

$$\frac{dM_Q}{dQ} \simeq m_{3/2}, \tag{11}$$

respectively [21,22].

In the usual scenario, the Q-ball is assumed to consist of only baryonic components such as $u^c d^c d^c$, but here if we consider the simple two-scalar model which consists of baryonic and leptonic components, whose more realistic case is $u^c u^c d^c e^c$, for example. Then, we can see that the baryonic component is stable against decay since $m_{3/2} < m_p$, and only the leptonic component can annihilate into e^+ inside Q-balls via gaugino and/or Higgsino exchange interactions. From this process, electric charge is induced in the Q-ball, and from Gauss's law, we see that $U(1)_{\mathrm{EM}}$ gauge field must have a classical configuration. In the next section, we consider the charged, or gauged Q-ball [8], which consists of not only the two scalars but also the $U(1)$ gauge field.

III. NEW TYPE OF CHARGED Q-BALL

A. Setup and basic properties

The Lagrangian of our two-scalar model is written as

$$\mathcal{L} = (D_\mu \Phi_B)^* D^\mu \Phi_B + (D_\mu \Phi_L)^* D^\mu \Phi_L$$
$$- V(\Phi_B, \Phi_L) - \frac{1}{4}F_{\mu\nu}F^{\mu\nu}, \tag{12}$$

$$D_\mu \Phi_B = (\partial_\mu - ieA_\mu)\Phi_B, \tag{13}$$

$$D_\mu \Phi_L = (\partial_\mu + ieA_\mu)\Phi_L, \tag{14}$$

and baryon and lepton charges are

$$B = \frac{1}{i} \int d^3x (\Phi_B^* D_0 \Phi_B - \Phi_B (D_0 \Phi_B)^*) \equiv \int d^3x b, \tag{15}$$
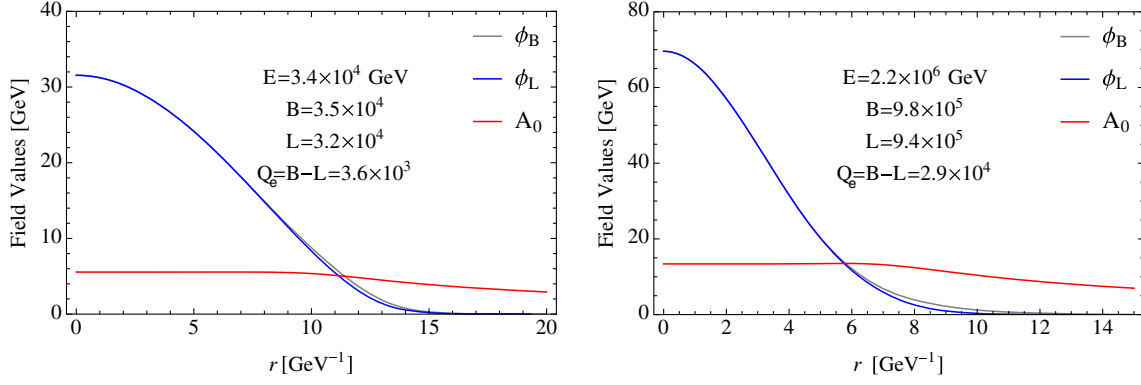
FIG. 1.   Examples of profiles of a charged *Q*-ball that has baryonic and leptonic components for a gauge-mediation-type charged *Q*-ball, with $m_\phi = 1$ GeV, and $e^2 = 0.002$ (left), and the new type of charged *Q*-ball, with $m_{3/2} = 1$ GeV, $|K| = 0.1$, and $e^2 = 0.002$ (right). They are slightly deformed from the neutral profiles, due to small nonzero electric charge.

$$L = \frac{1}{i} \int d^3x (\Phi_L^* D_0 \Phi_L - \Phi_L (D_0 \Phi_L)^*) \equiv \int d^3x l, \quad (16)$$

where b and l are baryon and lepton number densities. We assign the positive and negative electric charges for B and L components, respectively, and thus the total electric charge is given by

$$Q_e = B - L. \quad (17)$$

First, we set an ansatz on the configurations as follows[1]:

$$\Phi_i \equiv \frac{1}{\sqrt{2}} \phi_i, \qquad i = B, L \quad (18)$$

$$\phi_B(x, t) = e^{i\omega_B t} \phi_B(r), \quad (19)$$

$$\phi_L(x, t) = e^{i\omega_L t} \phi_L(r), \quad (20)$$

$$A_i = 0, \quad (21)$$

$$A_0 = A_0(r). \quad (22)$$

As reviewed in the previous section, there are simple expressions for energy, size, etc. of a neutral *Q*-ball, but for a charged *Q*-ball, the properties become difficult to analyze. However, in Ref. [7], we numerically found, for a gauge-mediation-type *Q*-ball, that the energy per unit charge is written as the neutral *Q*-ball expression plus coulomb potential at the surface of the *Q*-ball if the profile is not deformed very much,[2] as shown in Fig. 1:

$$\left(\frac{\partial E}{\partial B}\right)_L \simeq \left(\frac{\partial E}{\partial B}\right)_{L,\text{neutral}} + \frac{e^2 Q_e}{4\pi R}, \quad (23)$$

$$\left(\frac{\partial E}{\partial L}\right)_B \simeq \left(\frac{\partial E}{\partial L}\right)_{B,\text{neutral}} - \frac{e^2 Q_e}{4\pi R}, \quad (24)$$

where R denotes $R_B \simeq R_L$. The energy per unit charge is equal to the energy of a particle emitted from the *Q*-ball through the decay, we can interpret Eq. (24) that the energy of a particle emitted from the charged *Q*-ball is written as the energy coming from the residence inside of the *Q*-ball, plus the coulomb potential at the surface. This interpretation is consistent with the fact that the electric charge density mainly distributes at the surface of the *Q*-ball as shown in Fig. 2, which means that the charged particles are emitted from the surface.

In the case of the new type of *Q*-ball, however, the profile is Gaussian so the surface of the *Q*-ball must be defined carefully,[3] and we numerically found that the above expression does not hold when we naively regarded R given by Eq. (10) as the surface of the *Q*-ball. However, from the physical interpretation above, we can specify where the particles will be emitted from, and we can see from Fig. 2, that the electric charge is located at more outer region than R. We found that Eq. (24) still holds roughly for the new type of *Q*-ball as well when R is replaced by a larger value, which is shown in Fig. 3. The best fit is obtained when R is replaced by $\tilde{R} \equiv 2.5R$, and from now on we use Eq. (24) with R replaced by $\tilde{R}$. The plot is for $(\partial E/\partial B)_L = m_{3/2}$, $|K| = 0.1$, and $e^2 = 0.002$, but we confirmed the formula with $\tilde{R}$ for several values in the range $0.05 < |K| < 0.1$, $0.4 m_{3/2} < (\partial E/\partial B)_L < m_{3/2}$. From now on, we assume this analytic formula for the

[1]This parametrization is analogous to that of ordinary *Q*-ball, which is determined by the minimization of the energy for a fixed $U(1)$ charge, the definition of the Q-ball solution.

[2]In Ref. [7], we found that the realistic Q_e is very small compared to B or L, the deformation due to which is also small.

[3]As we see from Eq. (8), R is just defined to be the standard deviation.
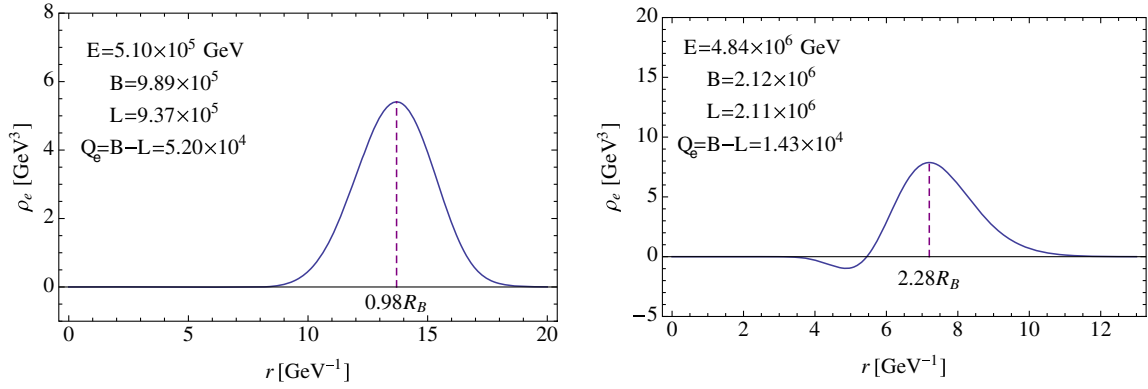
FIG. 2. Electric charge distributions of two-scalar charged Q-balls with small nonzero electric charge for a gauge-mediation-type charged Q-ball, with $m_\phi = 1$ GeV, and $e^2 = 0.002$ (left), and the new type of charged Q-ball, with $m_{3/2} = 1$ GeV, $|K| = 0.1$, and $e^2 = 0.002$ (right). We can see that the charge mainly distributes in the outer region, which, for the new type of charged Q-ball, is more outer than the standard deviation $R_B \simeq R_L$.

new type of charged Q-ball is valid for all parameter range we are interested in, and use it from the next section.

B. $Q_e^{(\mathrm{max})}$

Here we discuss maximum electric charge to which the Q-ball can be charged up by the decay. First of all, the condition $(\partial E/\partial L)_{B,\mathrm{neutral}} \simeq m_{3/2} > m_e$ must be satisfied for the decay to occur initially. As electric attraction grows, we expect that the emitted particle becomes bounded to the Q-ball, which means the energy of the emitted particle becomes smaller than the rest mass:

$$m_e > \left(\frac{\partial E}{\partial L}\right)_B = m_{3/2} - \frac{e^2 Q_e}{4\pi \tilde{R}} \qquad (25)$$

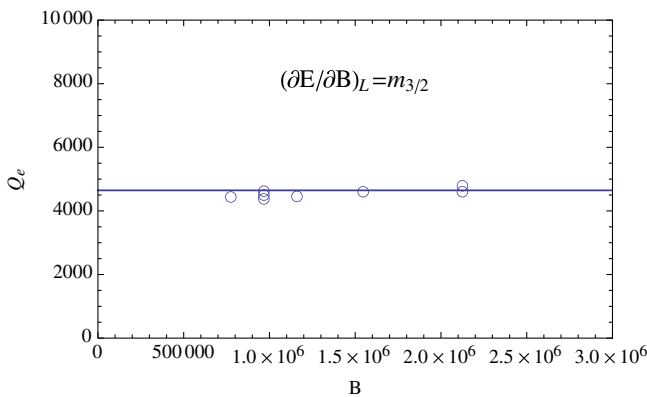$$= m_{3/2} - \frac{e^2 Q_e}{4\pi} \frac{1}{2.5|K|^{-1/2}m_{3/2}^{-1}}, \qquad (26)$$

FIG. 3. $B - Q_e$ plot for $(\partial E/\partial B)_L = m_{3/2}$. The dots are numerical result while the solid line indicates the analytic formula Eq. (24) with R replaced by $\tilde{R}$. We set $m_{3/2} = 1$ GeV, $|K| = 0.1$, and $e^2 = 0.002$.

thus

$$Q_e > 2.5\alpha^{-1}|K|^{-1/2}\left(1 - \frac{m_e}{m_{3/2}}\right) \qquad (27)$$

$$\simeq 2.5\alpha^{-1}|K|^{-1/2}, \qquad (28)$$

where we used Eq. (24) with R replaced by $\tilde{R}$, as mentioned in the previous section. As Q_e grows further, the Bohr radius becomes smaller, eventually than the Q-ball size. If we naively assume that the particle is absorbed into the Q-ball again in that case, the electric charge ceases to grow. The upper bound on the electric charge can be obtained as follows.

$$\frac{4\pi}{e^2 Q_e m_e} > \tilde{R} = 2.5|K|^{-1/2}m_{3/2}^{-1}, \qquad (29)$$

thus

$$Q_e < 2.5^{-1}\alpha^{-1}|K|^{1/2}\frac{m_{3/2}}{m_e}. \qquad (30)$$

Another effect which suppresses the growth of the electric charge is Schwinger effect, which states that if the electric field becomes large enough ($> E_{\mathrm{schwinger}} \sim m_e^2/e$), pair creation occurs at interval of Compton length. Therefore, if the electric field at the surface of the Q-ball becomes larger than $E_{\mathrm{schwinger}}$, the electron produced from pair creation is absorbed into the Q-ball, suppressing the growth of the electric charge. The upper bound on the electric charge in this case is obtained as follows.

$$E(\tilde{R}) = \frac{eQ_e}{4\pi\tilde{R}^2} < E_{\mathrm{schwinger}} = \frac{m_e^2}{e}, \qquad (31)$$

thus

$$Q_e < (2.5)^2 \alpha^{-1} |K|^{-1} \frac{m_e^2}{m_{3/2}^2}. \qquad (32)$$

The above argument applies when the Q-ball size is larger than the electron Compton length. If the size of the Q-ball is smaller than the Compton length, the electric charge can grow further until the electric field at Compton length becomes $E_{\text{schwinger}}$, since the pair creation occurs at interval of Compton length, so we obtain

$$E(1/m_e) = \frac{eQ_e}{4\pi} m_e^2 < E_{\text{schwinger}} = \frac{m_e^2}{e}, \qquad (33)$$

thus

$$Q_e < \alpha^{-1}, \qquad (34)$$

that is, the fine structure constant inverse ($\simeq 137$).

Finally, the electric repulsion may make the baryonic component unstable, so we must investigate whether the above upper bounds on the electric charge are still consistent with the stability condition. The baryonic component becomes unstable when the decay into nucleons becomes kinematically possible, which leads to the following stability condition:

$$m_p > \left(\frac{\partial E}{\partial B}\right)_L = m_{3/2} + \frac{e^2 Q_e}{4\pi \tilde{R}}, \qquad (35)$$

thus

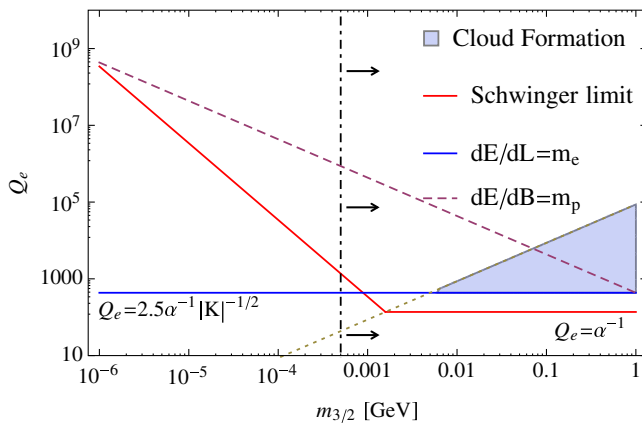$$Q_e < 2.5 \alpha^{-1} |K|^{-1/2} \left(\frac{m_p}{m_{3/2}} - 1\right) \qquad (36)$$

FIG. 4. Upper bounds on electric charge of the new type of charged Q-ball. The dotted line indicates when Q-ball size becomes equal to the Bohr radius, and the dashed-dotted line is $m_{3/2} = m_e$, whose right side is allowed. We have used $|K| = 0.1$.

$$\simeq 2.5 \alpha^{-1} |K|^{-1/2} \frac{m_p}{m_{3/2}}. \qquad (37)$$

Therefore, the growth of electric charge must stop before it reaches the upper bound given by Eq. (37). In Fig. 4, we illustrate the full upper bound on the electric charge of the Q-ball, and show that it safely maintain the stability of the baryonic component.

IV. PRESENT RELICS AND MICA CONSTRAINT

Here we discuss the present relics from the new type of charged Q-balls and their detections. We focus on the case that the Bohr radius is larger than the Q-ball size when maximally charged up, so that we can treat the charged Q-ball as ordinary nucleus with extremely heavy mass, which makes the analysis easier. We see from Fig. 4, that this condition is given by

$$m_{3/2} > |K|^{-1/2} m_e, \qquad (38)$$

and electric charge becomes $Q_e = \alpha^{-1}$. Then, the charged Q-balls captures the other charged particles like ordinary nucleus, which was already analyzed in Ref. [14]. There, we used Saha's equation to roughly estimate when the recombination starts, that is, when $n_{1S}/n_{\text{Q-ball}} \sim 1$ (n_{1S}: number density of bound state of a Q-ball and an electron), and we found that the recombination temperature becomes $T_{\text{rec}} \simeq 8.6$ keV, if we use, as binding energy, the usual value of nucleus and electron. Similarly, we could find when the recombination finishes, that is, when the charged Q-ball completely neutralizes. Since binding energy decreases due to the screening effect of the orbiting electrons for large enough elements, the neutralization temperature necessarily becomes smaller than the usual proton-electron recombination temperature. Therefore, the Q-balls do not neutralize, since the free electrons are already captured by protons. Thus, we can conclude that, if charged Q-balls with $Q_e \sim \alpha^{-1}$ are formed well before the BBN epoch, the present relics become $+O(1)$ ionlike extremely heavy objects. These relics must eventually account for dark matter of the Universe, i.e.,

$$\frac{\rho_{\text{Q-ball}}}{s} = \frac{\rho_{\text{DM}}}{s} \simeq 4.4 \times 10^{-10} \text{ GeV}, \qquad (39)$$

where ρ_{DM} and s are the dark matter energy density and entropy density in the present Universe, respectively.

The ionlike relics experience electromagnetic processes. Thus, experiments sensitive to those processes are applicable, and nondetection of the processes gives upper bounds on the amount or flux of the objects. Various upper bounds on the flux of the charged Q-ball relics are obtained in Ref. [9], and the most stringent comes from the MICA experiment [13],

$$F \lesssim 2.3 \times 10^{-20} \text{ cm}^{-2} \text{ s}^{-1} \text{ sr}^{-1}, \qquad (40)$$

where they did not observe any trails of the heavy ionlike object in 10^9 year-old ancient muscovite mica crystals. The constraint is severe, mainly due to the long detection time, which is essentially the age of the mica. The other features are discussed in Ref. [14], along with the application on the gauge-mediation-type Q-ball case. Since the Q-ball is so heavy that the orbiting particles virtually have no effect on total mass, the dark matter flux is given by

$$F \simeq \frac{\rho_{\text{DM}\odot}}{M_Q} v, \qquad (41)$$

where $\rho_{\text{DM}\odot}$ denotes dark matter energy density near the Solar System, and v is the virial velocity of the Q-balls. Therefore, using $\rho_{\text{DM}\odot} \sim 0.3 \text{ GeV/cm}^3$ and $v \sim 10^{-3}$, we obtain the following constraint on the mass of the Q-ball:

$$M_Q \gtrsim 3.9 \times 10^{26} \text{ GeV}. \qquad (42)$$

This is a severe constraint, which easily reaches the typical mass of the Q-ball, and it constrains ϕ_{osc} via Eq. (7). We can translate it into the condition on $m_{3/2}$ and the reheating temperature T_{RH}, using a relation of ϕ_{osc} and reheating temperature T_{RH} given by

$$\frac{\rho_{\text{DM}}}{s} \sim \frac{3 T_{\text{RH}}}{4} \frac{M_Q n_\phi / Q}{3 H_{\text{osc}}^2 M_{\text{P}}^2} \sim \frac{9}{4} T_{\text{RH}} \frac{\phi_{\text{osc}}^2}{M_{\text{P}}^2}, \qquad (43)$$

where $n_\phi = m_{\text{eff}} \phi_{\text{osc}}^2$, $3 H_{\text{osc}} \simeq m_{\text{eff}}$, $m_{\text{eff}} \simeq m_{3/2}$, and Q is global charge ($= B + L$ for the model considered in Sec. III A) of the Q-ball. We used Eq. (9) [20]. Inserting the observational value $\rho_{\text{DM}}/s \simeq 4.4 \times 10^{-10} \text{ GeV}$ [23], we obtain

$$\phi_{\text{osc}} \simeq 4.75 \times 10^{13} \text{ GeV} \left(\frac{T_{\text{RH}}}{\text{GeV}}\right)^{-1/2}. \qquad (44)$$

Using this relation and Eq. (7), Eq. (42) is rewritten as

$$T_{\text{RH}} \lesssim 5.79 \times 10^0 \left(\frac{m_{3/2}}{\text{GeV}}\right)^{-1} \text{ GeV}, \qquad (45)$$

which is a condition on $m_{3/2}$ and T_{RH}.

In Fig. 5, we show the allowed parameter region of $m_{3/2}$ and T_{RH}, using the analogous method to that in Ref. [11], where the authors applied the IceCube constraint on the neutral Q-ball dark matter. The MICA constraint Eq. (45) corresponds to the magenta solid line in the figure.

The horizontal dotted lines indicate the condition that the gravity mediation effect dominates the potential of the Q-ball, which is given by Eq. (6). Using Eq. (44), the condition is written as
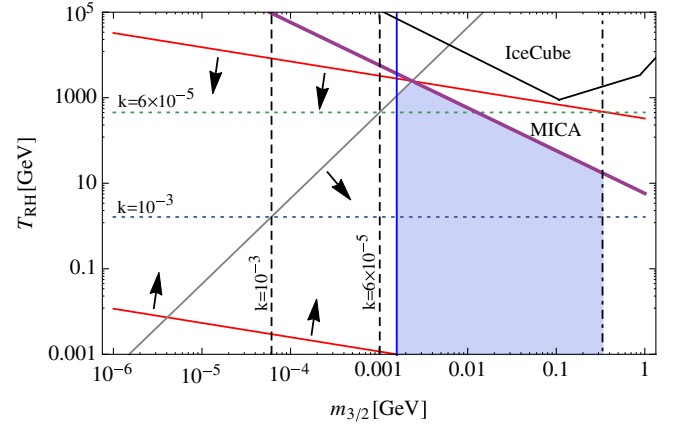

FIG. 5. Allowed region for the new type of charged Q-ball as the dark matter (shaded region). The thick line shows the upper bound Eq. (42), the dotted lines denote the lower bound Eq. (46) for each value of k shown, the dashed line corresponds to the Λ_{mess}-limit Eq. (50) with $g = 1$, for each value of k shown, the dashed-dotted line is the upper bound Eq. (37) for $Q_e = \alpha^{-1}$, and the blue line represents the lower bound Eq. (38). The bounds from Affleck-Dine mechanism are illustrated by red lines, and arrows are directed towards allowed region. The IceCube constraint is also represented at the upper right [11].

$$T_{\text{RH}} \lesssim 1.63 \times 10^{-6} \text{ GeV} g^{-2} k^{-2}. \qquad (46)$$

In Fig. 5, the upper bounds on T_{RH} for $k = 6 \times 10^{-5}$ and 10^{-3} are shown.

Another condition on gravitino mass (SUSY breaking scale) comes from the observation value of Higgs boson mass at around 126 GeV [15,24]:

$$\Lambda_{\text{mess}} \equiv \frac{kF}{M_{\text{mess}}} \gtrsim 5 \times 10^5 \text{ GeV}. \qquad (47)$$

Since the SUSY breaking scale is typically assumed to be small compared to the messenger mass,

$$kF < M_{\text{mess}}^2, \qquad (48)$$

Eq. (47) becomes

$$\sqrt{kF} \gtrsim 5 \times 10^5 \text{ GeV}. \qquad (49)$$

Then, using Eq. (5), it reduces to

$$m_{3/2} \gtrsim 6.1 \times 10^{-8} k^{-1} \text{ GeV}, \qquad (50)$$

which corresponds to the vertical dashed line in Fig. 5.

The dashed-dotted line in Fig. 5 indicates stability condition Eq. (37) for $Q_e = \alpha^{-1}$. Finally, as mentioned in the beginning of the section, since we are considering the Q-ball smaller than the Bohr radius so that the potential the external particles experience can be approximated into Coulomb-type potential, Eq. (38) must be satisfied, which

corresponds to the thin line in Fig. 5. The IceCube constraints, which are relevant only to the KKST process, are shown for comparison, and we see that a more stringent MICA constraint makes the allowed region smaller.

By far, we treated the AD field at the onset of oscillation ϕ_{osc} as a free parameter. However, since the dynamics of AD field is essentially governed by the balance between the negative Hubble induced mass term and higher-dimensional operator in the superpotential $W \sim \phi^n/M^{n-3}$, ϕ_{osc} is determined as

$$\phi_{osc} \sim (H_{osc} M^{n-3})^{1/(n-2)} \tag{51}$$

$$\sim (m_{eff} M^{n-3})^{1/(n-2)} \tag{52}$$

$$= (m_{3/2} M^{n-3})^{1/(n-2)}, \tag{53}$$

where we used $H_{osc} \sim m_{eff} = m_{3/2}$, due to the gravity mediation domination in the AD potential. Thus, we investigate whether the AD mechanism actually can generate the viable amplitude of the AD field, so that it is consistent with the constraints discussed above. Specifically, we examine whether the reheating temperature determined by Eq. (44) and Eq. (53),

$$T_{RH} \sim 2.26 \times 10^{27}\, \text{GeV} \left(\frac{m_{3/2}}{\text{GeV}}\right)^{-2/(n-2)} \left(\frac{M}{\text{GeV}}\right)^{-2(n-3)/(n-2)}, \tag{54}$$

is consistent with the allowed region in Fig. 5, for viable n and M. Since we are considering $u^c u^c d^c e^c$ instead of the usual $u^c d^c d^c$, n becomes different from when we consider the neutral Q-ball. We take $n = 8$ since $n = 4$ is unfavored from proton decay, while for $u^c d^c d^c$, we must take $n = 6$, for instance. Then, we find that Eq. (54) is consistent with the allowed region for $4.16 \times 10^{-4} M_P < M < 3.07 M_P$, which is a reasonable range for M, whose bounds are illustrated by red lines in Fig. 5.

V. CONCLUSIONS AND DISCUSSION

In gauge mediation models, the gravity mediation effect can still dominate over the gauge mediation effect in the scalar potential if the field value is large. In that case, the new type of Q-balls, which have different properties from gauge-mediation-type Q-balls, are formed after the Affleck-Dine baryogenesis. The new type of Q-ball has property that it is stable against the decay into baryons but it can decay into leptons lighter than gravitino. Therefore, the new type of Q-balls that carry both baryon and lepton charges can be electrically charged due to the leptonic decay only, which are called charged or gauged Q-balls [8]. Also, they are stable by virtue of the stability of the baryonic component, thus, the new type of charged Q-ball

can be a viable candidate for dark matter in the present Universe. In this paper, we examined the allowed parameter region for the new type of charged Q-ball dark matter. We focused on the case where the charged Q-ball can be treated as ordinary nucleus, in order to simplify the analysis. Then, we found that electric charge of charged Q-balls becomes $Q_e \sim \alpha^{-1}$, and the present relics of them become $+O(1)$ ionlike extremely heavy objects. The relics can be treated as ordinary ions, so they are detectable by the MICA experiment, where no trail of heavy ionlike object is observed in 10^9 year-old ancient mica crystals. This gives the stringent constraint on the dark matter flux since the detection time, which is the age of the mica crystals, is extremely long. We translated the constraint into that on the gravitino mass $m_{3/2}$ and reheating temperature T_{RH}, as done in Ref. [11] for the IceCube constraint on the neutral Q-ball dark matter. As a result, we found that the MICA constraint makes the allowed region in $m_{3/2}$—T_{RH} smaller. The constraint from the High Altitude Water Cherenkov (HAWC) Observatory will be of future interest since it is expected to give a strong bound compared to Super-Kamiokande or MACRO, for instance, due to its greater volume [25].

Since the dynamics of the AD field is essentially governed by the AD potential, ϕ_{osc} is actually not a free parameter and determined by the balance between the negative Hubble induced mass term and the higher-dimensional operator in the superpotential $W \sim \phi^n/M^{n-3}$. We examined whether the amplitude of the AD field allowed by the constraints in Fig. 5 is actually generated. Since the realistic example of the flat direction in our case is $u^c u^c d^c e^c$, instead of the usual $u^c d^c d^c$ for the AD baryogenesis, n becomes different from the latter. We took $n = 8$, since $n = 4$ is unfavored from proton decay, while for $u^c d^c d^c$, $n = 6$ is taken, for instance. We found the parameter range $4.16 \times 10^{-4} M_P < M < 3.07 M_P$ is consistent with the allowed region in Fig. 5, which is a viable range for M.

We found that the flat direction which forms charged Q-balls can explain dark matter in the Universe, but the number of baryonic particles emitted from evaporation of the charged Q-ball due to thermal bath is too small to explain the baryon asymmetry in the Universe [26]. However, by using another flat direction, the baryon asymmetry can be explained as well.

We focused on the region where the charged Q-ball can be treated as an ordinary nucleus, which means the Bohr radius is larger than the Q-ball size. For the opposite case, where the Bohr radius is smaller than the Q-ball size, we naively assumed in Sec. III B, that the emitted particle is absorbed again into the Q-ball, which suppresses the further growth of electric charge. However, the physics when the Bohr radius is smaller than the Q-ball size may be a complex issue. For example, the particle may orbit inside of the Q-ball, experiencing the different potential from Coulomb type. Then the bound state with different

properties including binding energy may be formed, which will change the present relics. Then, the detections may have to be applied differently as well. It will be a future task to investigate what will happen when the orbit is smaller than the Q-ball size.

We assumed the $u^c u^c d^c e^c$-like B and L flat direction which includes only the electron as the leptonic component. However, if we consider the direction which consists of the neutrino component, for example $QQQL$, the scenario may be significantly different. For instance, due to the decay channel into neutrinos, the Q-ball may have $SU(2)$ charge, and a fundamental theory of the non-Abelian gauged Q-ball may need to be considered.

[1] I. Affleck and M. Dine, Nucl. Phys. **B249**, 361 (1985); M. Dine, L. Randall, and S. D. Thomas, Phys. Rev. Lett. **75**, 398 (1995); Nucl. Phys. **B458**, 291 (1996).

[2] A. Kusenko and M. Shaposhnikov, Phys. Lett. B **418**, 46 (1998).

[3] S. Kasuya and M. Kawasaki, Phys. Rev. D **61**, 041301 (2000).

[4] S. Kasuya and M. Kawasaki, Phys. Rev. D **62**, 023512 (2000).

[5] S. Coleman, Nucl. Phys. **B262**, 263 (1985).

[6] G. Dvali, A. Kusenko, and M. Shaposhnikov, Phys. Lett. B **417**, 99 (1998).

[7] J. Hong, M. Kawasaki, and M. Yamada, Phys. Rev. D **92**, 063521 (2015).

[8] K. Lee, J. A. Stein-Schabes, R. Watkins, and L. M. Widrow, Phys. Rev. D **39**, 1665 (1989).

[9] J. Arafune, T. Yoshida, S. Nakamura, and K. Ogure, Phys. Rev. D **62**, 105013 (2000).

[10] Y. Takenaga *et al.* (Super-Kamiokande Collaboration), Phys. Lett. B **647**, 18 (2007).

[11] S. Kasuya, M. Kawasaki, and T. T. Yanagida, Prog. Theor. Exp. Phys. **2015**, 53B02 (2015).

[12] A. Kusenko, V. Kuzmin, M. E. Shaposhnikov, and P. G. Tinyakov, Phys. Rev. Lett. **80**, 3185 (1998).

[13] P. B. Price and M. H. Salamon, Phys. Rev. Lett. **56**, 1226 (1986); D. Ghosh, and S Chatterjea, Europhys. Lett. **12**, 25 (1990).

[14] J. Hong, M. Kawasaki, and M. Yamada, J. Cosmol. Astropart. Phys. 08 (2016) 053.

[15] K. Hamaguchi, M. Ibe, T. T. Yanagida, and N. Yokozaki, Phys. Rev. D **90**, 015027 (2014).

[16] M. Dine, W. Fischler, and M. Srednicki, Nucl. Phys. **B189**, 575 (1981); S. Dimopou- los and S. Raby, Nucl. Phys. **B192**, 353 (1981); M. Dine and W. Fischler, Phys. Lett. B **110B**, 227 (1982); Nucl. Phys. **B204**, 346 (1982); C. R. Nappi and B. A. Ovrut, Phys. Lett. B **113B**, 175 (1982); L. Alvarez-Gaume, M. Claudson, and M. B. Wise, Nucl. Phys. **B207**, 96 (1982).

[17] M. Dine and A. E. Nelson, Phys. Rev. D **48**, 1277 (1993); M. Dine, A. E. Nelson, and Y. Shirman, Phys. Rev. D **51**, 1362 (1995); M. Dine, A. E. Nelson, Y. Nir, and Y. Shirman, Phys. Rev. D **53**, 2658 (1996).

[18] A. de Gouve'a, T. Moroi, and H. Murayama, Phys. Rev. D **56**, 1281 (1997).

[19] K. Enqvist and J. McDonald, Nucl. Phys. **B538**, 321 (1999).

[20] S. Kasuya and M. Kawasaki, Phys. Rev. D **64**, 123515 (2001).

[21] J. Hisano, M. M. Nojiri, and N. Okada, Phys. Rev. D **64**, 023511 (2001).

[22] M. Kawasaki and M. Yamada, Phys. Rev. D **87**, 023517 (2013).

[23] P. A. R. Ade *et al.* (Planck Collaboration), Astron. Astrophys. **571**, A16 (2014).

[24] J. L. Feng, Z. Surujon, and H. B. Yu, Phys. Rev. D **86**, 035003 (2012).

[25] HAWC Collaboration, arXiv:1310.0073.

[26] S. Kasuya and M. Kawasaki, Phys. Rev. D **89**, 103534 (2014).